NUMERICAL FORMULATION OF SEA LOADS TO IMPERMEABLE NETS

Are Johan Berstad*, Line Fludal Heimstad†

Aquastructures
Kjøpmannsgata 21, 7013 Trondheim, Norway
e-mail: mail@aquastructures.no
web page: http://www.aquastructures.no

Key words: Numerical calculations, impermeable nets, AquaSim, Finite Element analysis.

Abstract. A load formulation has been introduced to the Finite Element program AquaSim, where the net is impermeable and water is hence not allowed to pass through the elements belonging to the impermeable net. This paper presents the theory of the load formulation, and presents three case studies where the load model is validated.

1 INTRODUCTION

The aquaculture industry has increased rapidly the last 30 years. In almost all fish farms, the fish is held contained in net cages. In 2009, the Norwegian standard, NS 9415, was revised, and in 2011 corresponding regulations were enforced. This largely increased the number of analysis being carried out on aquaculture structures.

Lice on farmed fish in Norway has increased concurrently with the growth of the aquaculture industry. In order to maintain the growth and the sustainability, the industry is forced to come up with solutions. Two suggestions, which is believed to reduce and perhaps eliminate lice on farmed fish, are closed flexible bags or stiffer structures and Lice-skirts mounted on the upper part of the net.

Common with both of these suggestions is that water can not flow through the net, since the material is impermeable. This introduces a significant change to the governing physics, where the usual Morison type load formulation applied to groups of twines is no longer applicable. The structure will behave as a large floating mass being withheld inside a thin sheet. The current is forced to flow around, and the waves are accompanied by diffraction or deformation of the impermeable net.

This paper presents the load formulation that has been introduced to the computer program AquaSim [1, 2, 3] for analysis to impermeable nets. AquaSim is a FE computer program used for the design of almost all fish farm systems in Norway, and is also in wide use in other countries doing offshore fish farming such as Chile and Australia.

2 THEORETICAL FORMULATION

2.1 Internal pressure and static equilibrium

Consider a tank filled with an arbitrary fluid. The tank can also be empty. Assume that the fluid inside the tank has a different water level than the fluid outside the tank as shown in Fig. 1.
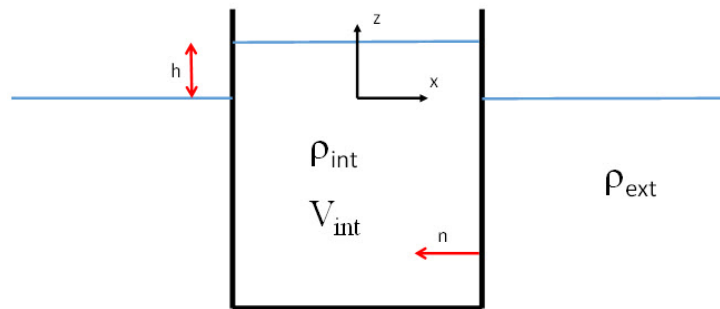
Figure 1: Tank in water

The tank has an inside volume, V_{int}. Load equilibrium for a net panel of the tank is found as:

$$F_n = gzA(\rho_{ext} - \rho_{int}) - ghA\rho_{int} \tag{1}$$

Where F_n is the normal force to a net panel pointing into the tank where a net is subdivided into several panels. More abbreviations is found at the end of this document. Positive value of h means the water level inside the tank is higher than the water level outside the tank. If the tank is empty the inside water density, ρ_{int}, will be zero.

Figure 2a and 2b shows a case were the inside water density is the same as the outside water density, but the water height, h, inside is one meter above the water level outside the cage. In this cage the inside pressure leads to a deformation of the net going outwards (x-direction) and downwards (z-direction). Whether the net is deformed, or the cage moves downwards is decided by the stiffness of the net, relative to the stiffness of the water plane area.

(a) x-direction

(b) z-direction
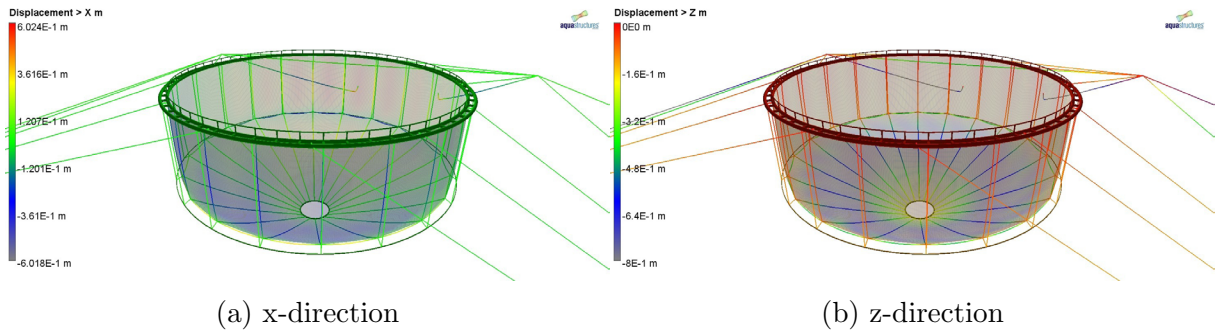
Figure 2: Deformation of the net. Inside water lever is one meter above the outside water level

2.2 Forces from current flow around cylinder

Impermeable nets may also be open at the top and at the bottom. For example skirts to avoid lice, i.e. lice skirts. This is shown in Fig. 3. In this case, the static pressure inside will be equal to the static pressure outside the net.
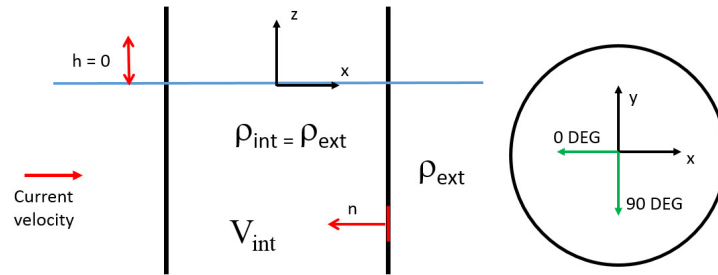
Figure 3: Dense net in current flow.

Consider a current velocity approaching along the x-axis. The current flow around a cylinder will introduce a velocity field which introduces a pressure field to the cylinder.

The pressure field around a cylinder is implemented to AquaSim in a simplified way as shown in Fig. 4. A drag and a lift coefficient is introduced. The pressure coefficient, C_p, upstream may be expressed as:

$$C_p = 1 - (C_l + 1)\sin^4\theta, \quad \text{for} \quad 0° \leq \theta \geq 90° \tag{2}$$

Note that this corresponds to the analytical solution for an inviscid flow with $C_l = 3.0$. C_p at the leeward side of the cylinder is found as:

$$C_p = min(1 - (C_l + 1)\sin^4(90 + (\theta - 90) \cdot 1.5) - C_{wake} \tag{3}$$

Where C_{wake} is found by matching the overall drag to the cylinder, to the drag force derived from the input drag and lift coefficients.
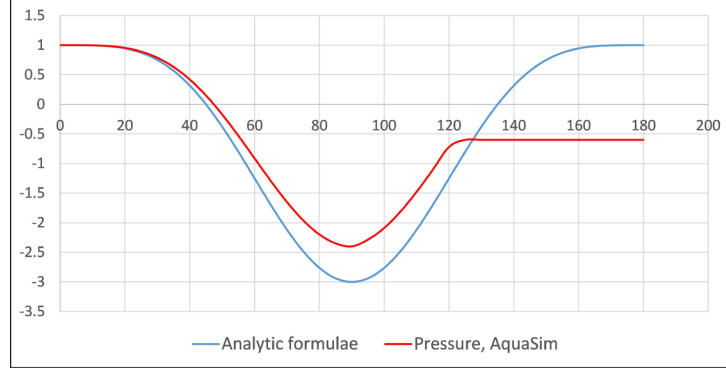
Figure 4: Pressure distribution around a cylinder as calculated in AquaSim.

Having found C_p as a function of the angle between the element in the horizontal plane, and the current flow the force acting on a net panel with an area, A, is found as:

$$F_n = \frac{\rho A C_p}{2} U_c^2 \tag{4}$$

The cross-flow principle is applied such that the U_c is the part of the current velocity normal to the element at the element fronting the current direction.

In addition a skin friction force, F_s, can be applied and may be expressed as:

$$F_s = \frac{\rho A C_s}{2} U_{tan}^2 \tag{5}$$

The skin friction part of the force is applied for the current flow in the tangential direction, both circumferential and along the length of the cylinder.

2.3 Wave force

For wave forces the pressure from the incident wave, i.e. Froude-Kriloff, and the pressure caused by the wave diffraction are calculated according to MacCamy and Fuchs theory [6].

In a regular sea with airy waves, the dynamic pressure from the incident wave is found as [4]

$$p_{FC} = \rho g \zeta \frac{\cosh k(z + h)}{\cosh kh} \sin(\omega t - kx) \tag{6}$$

For an irregular sea state the expression for the dynamic pressure is [4]:

$$p_{MF} = \sum_{n=1}^{N} \rho g \zeta_n \frac{\cosh k_n(z + h)}{\cosh k_n h} \sin(\omega_n t - k_n x + \epsilon_n) \tag{7}$$

In Eq. 7 N sinusoidal wave components are used to represent the wave spectrum, n means the nth sinusoidal wave component and ϵ_n is a random phase for each sinusoidal wave component.

The pressure caused by a diffracted wave around the surface of the cylinder with a radius r, according to [6] is:

$$p_{MF} = \rho g \zeta \frac{\cosh k(z+h)}{\cosh kh} \sum_{n=0}^{\infty} i[B_n H_n^1(kr)] \cos n\theta e^{-i\omega t} \tag{8}$$

Where:

$$B_n = -\epsilon_n i^n \frac{J'(kr)}{H^{(1)}(kr)} \tag{9}$$

In an irregular sea the pressure from the diffracted wave field along the surface is found as:

$$p_{MF} = \sum_{m=1}^{N} \rho g \zeta_m \frac{\cosh k_m(z+h)}{\cosh k_m h} \sum_{n=0}^{\infty} i[B_n H_n^1(kr)] \cos n\theta e^{-i\omega t + \epsilon_n} \tag{10}$$

The total pressure at a given point is then found as:

$$p = p_{FC} + p_{MF} \tag{11}$$

As the MacCamy and Fuchs theory for diffracted waves is valid for vertical cylinders, ρ_{MF} is multiplied with the vertical projection of the area. For instance, as a traditional net deforms in waves the pressure from a diffracted wave, according to MacCamy and Fuchs theory, will be lower as it will in reality as well. AquaSim aims at being on the conservative side.

2.3.1 Wave drift

Drift forces is proportional to the wave elevation squared and is hence a 2nd order effect. It should therefore be found keeping all 2nd order terms of the force in a 2nd order perturbation approach. The wave potential may be expressed as [4]:

$$\phi = \phi_1 + \phi_2 \tag{12}$$

Where ϕ_1 is the 1st order potential and ϕ_2 is the 2nd order potential. Latter will not give any contribution to drift forces [4]. Hence, drift forces is found by keeping the 2nd order terms when evaluating the Bernoulli equation in the 1st order potential, given as:

$$p = \rho g z - p \frac{\partial \phi_1}{\partial t} - \frac{\rho}{2} \left\{ \left(\frac{\partial \phi_1}{\partial x} \right)^2 + \left(\frac{\partial \phi_1}{\partial y} \right)^2 + \left(\frac{\partial \phi_1}{\partial z} \right)^2 \right\} \tag{13}$$

Also, 2nd order terms with a zero mean force can be omitted. Following [4] the terms given in Eq. 14 and Eq. 15, of the 1st order potentials, are the ones contributing to drift forces:

$$p = -\rho g \int_0^\zeta z dz - p \frac{\partial \Phi_1}{\partial t}|_{z=0\zeta} \tag{14}$$

and:

$$-\frac{\rho}{2} \int_{-\infty}^0 \left\{ \left(\frac{\partial \phi_1}{\partial x}\right)^2 + \left(\frac{\partial \phi_1}{\partial y}\right)^2 + \left(\frac{\partial \phi_1}{\partial z}\right)^2 \right\} dz \tag{15}$$

Which corresponds to the velocity squared term in the Bernoulli equation, and also give contribution to the drift force. Equation 14-15 are valid for infinitely deep cylinders. For the real case the cylinders integrals are performed from the bottom of the cylinders, as the lowest point.

It should be noted that by including the drift terms from Eq. 14 and Eq. 15 also a sum frequency load is introduced to the analysis. This is not the full sum frequency load effect, but only parts contributing to drift.

3 CASE STUDIES

3.1 Wave and current forces to cylinder

Two cylinder-shaped models have been established in AquaSim: One consisting of beam elements, and the other with impermeable membrane elements covering the circumference. Both models with the parameters given in Tab. 1. The length of the cylinders is situated vertically, i.e. in the negative z-direction from the sea surface and downwards, as shown in Fig. 5. The cylinder is kept from moving such that the velocity of the cylinder itself is negligible, and the wave length is large relative to the cylinder diameter. The long wave approximation [4] should give good results in this case, meaning that the results from these two models should have good correspondence.

Table 1: Cylinder particulars

Diameter [m]	4
Depth [m]	15
$\rho_w \ [\frac{kg}{m^3}]$	1025
C_d	1.2
ζ [m]	5
T [s]	10
$U_c \ \frac{m}{s}$	1.0
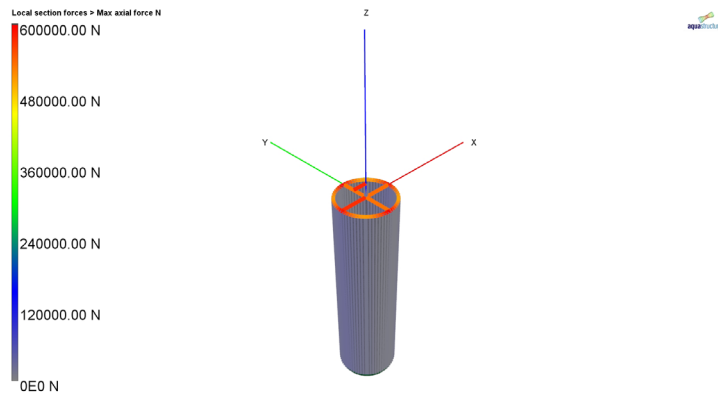
Figure 5: Vertical cylinder.

The Morrison equation [7], for a non-moving object, can be expressed as:

$$F = \rho C_m V \dot{u} + \rho C_d A u |u| \tag{16}$$

Where the first term in Eq. 16 is the inertia forces, and the second term is the drag forces.

3.1.1 Current loads

Figure 6 shows comparison between the Net model and the Beam model exposed to current only, and with three different drag coefficients, i.e. $C_d = 0.6$, $C_d = 1.2$ and $C_d = 2.0$. In this case, only the drag forces from Eq. 16 will apply. As seen from this figure there is a good correspondence between the results.
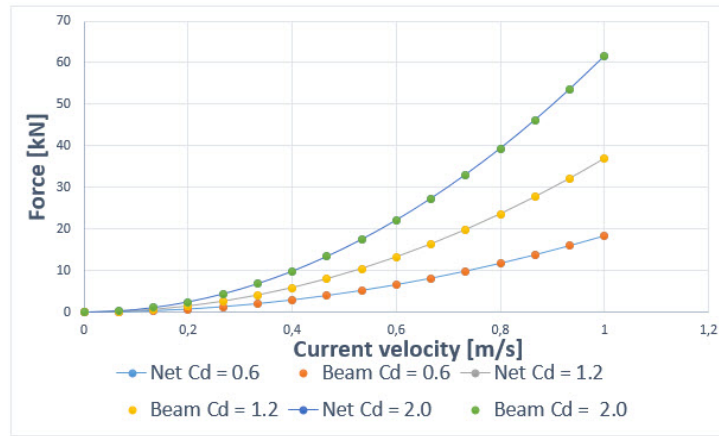
Figure 6: Comparison between the Net and Beam model exposed to current, and with different drag coefficients.

3.1.2 Wave and current loads

The inertia part of the forces is the results of the pressure distribution around the object, where F in the direction i can be expressed as:

$$F_i = \iint_S pn_i ds + am_{i1}a_1 + am_{i2}a_2 + am_{i3}a_3 \qquad (17)$$

Where n_i is the normal vector pointing into the object. For a case where the wave is long relative to the volume, the divergence theorem can be expressed as:

$$F_1 = \rho V a_1 + am_{11}a_1 = \rho V(a_1 + a_1) = \rho V(1 + C_a)a_1 = \rho V C_m a_1 \qquad (18)$$

For long waves the MacCamy and Fuchs theory should asymptotically lead to the same results as Eq. 18 with $C_m = 2.0$. The results with the Net and the Beam model, exposed to wave and current, are shown in Fig. 7. As seen from this figure there is a good correspondence between the results.
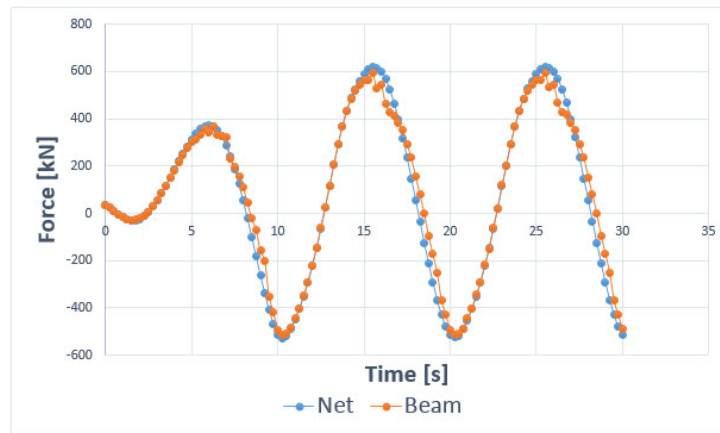
Figure 7: Net model and beam model exposed to wave and current.

3.2 Current forces to impermeable net - lice skirt

The load model implemented in AquaSim for impermeable net has been compared to model experiments performed by [5]. The impermeable net has a depth of 0.540 m, and the current velocity is in the range $U_c = 0.05 - 0.20 m/s$. Both the top and the bottom of the lice skirt is open (See Fig. 3). The numerical model from AquaSim is shown in Fig. 8. The current is applied along the positive x-axis.
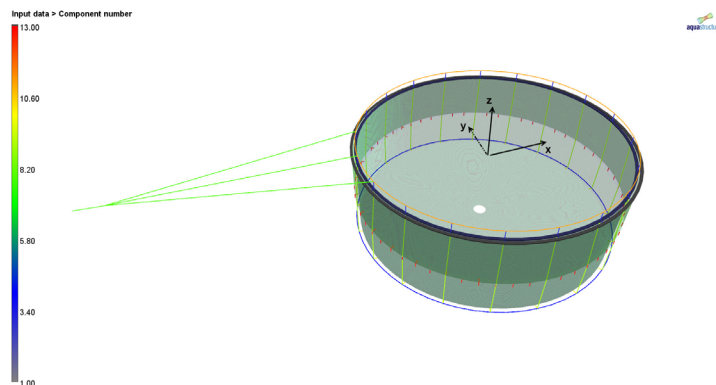
Figure 8: Numerical model in AquaSim with liceskirt.

The numerical results has been compared to the experimental results using a $C_d = 1.2$, and a $C_l = 2.0$. Four different values for C_f has been used, i.e. $C_f = 0.00$, $C_f = 0.12$, $C_f = 0.18$ and $C_f = 0.24$. The results are shown in Fig. 9.
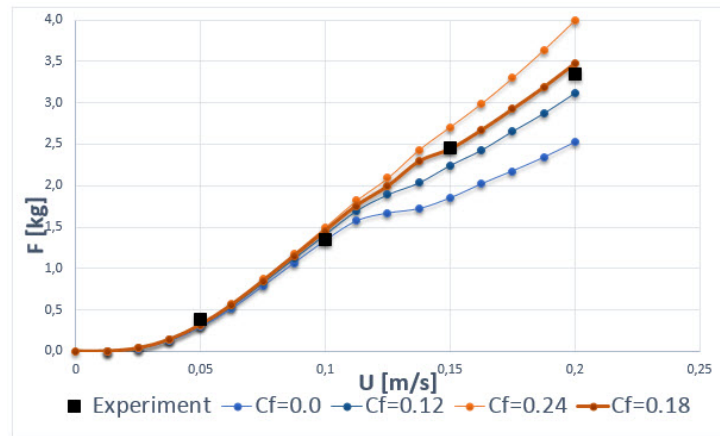
Figure 9: Numerical results compared to model experiments from [5], with $C_d = 1.2$, $C_l = 2.0$ and four different values for C_f.

3.3 Wave forces and response to SPAR buoy

Figure 10 shows two variations of a SPAR buoy modelled in AquaSim. In the Beam model the properties are distributed to beam elements. The properties includes load application from Morison's formulae [7] and added mass. For load application the Morison's formulae is applied for the beam with added mass coefficient of $C_a = 1.0$, giving a $C_m = 2.0$. For the Net model a net is put along the circumference of the cylinder. Loads are calculated on the net from MacCamy Fuchs theory [6]. Added mass is placed on the net giving the same added mass as for Model 1.

(a) Beam model (b) Net model
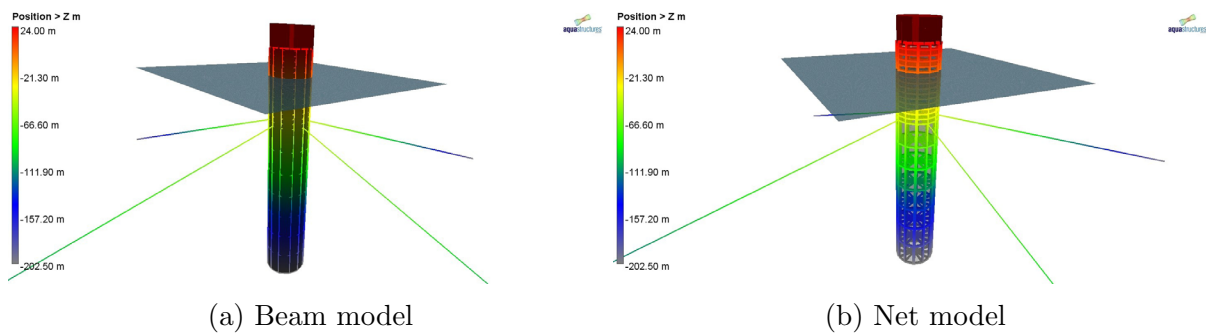
Figure 10: SPAR buoy

The main data for the analysed case, in both the Beam and the Net model, is given in Tab. 2.

Two variations of the Net model has been carried out: One where all load components, contributing to slow varying drift forces, are accounted for, and one Net model where 1st order forces are calculated to the actual free surface. The models are:

Table 2: Particulars regarding the SPAR Buoy

Environment	
Wave amplitude [m]	5.0
Wave period [s]	22.6
SPAR buoy	
Diameter [m]	37.5
Depth [m]	200.0
COG	-102.5
COB	-100.0
Mass of structure [ton]	225435
Horizontal added mass [ton]	226416
Vertical added mass [ton]	0
Moorings	
Horizontal length [m]	481.25
Depth [m]	202.5
EA [kN]	170112
Pretension [kN]	4888
Weight per meter [kg/m]	185
Eigen period system	
Heave	28
Surge/sway [s]	219
Pitch/roll [s]	94
Yaw	Suppressed

1. Beam model: All properties are distributed to a beam. Loads are calculated to the actual free surface, as shown in Eq. 14.

2. Net model with drift: A net is wrapped around the beams. All hydrodynamic loads are applied to the net, and not to the beam. The properties regarding the buoyancy are the same as for the Beam model. In addition to integrating to the free surface, Eq. 14, the load term of Eq. 15 is included.

3. Net model without drift: In this case the load term from Eq. 15 is not included, but all other load terms are the same.

A drag coefficient of $C_d = 1.2$ is applied to all the beam and membrane elements. For the mooring lines, a drag coefficient of $C_d = 1.3$ and a drag diameter of 142 mm has been applied.

The results from the analysis in AquaSim are shown in Fig. 11 and Fig. 12.
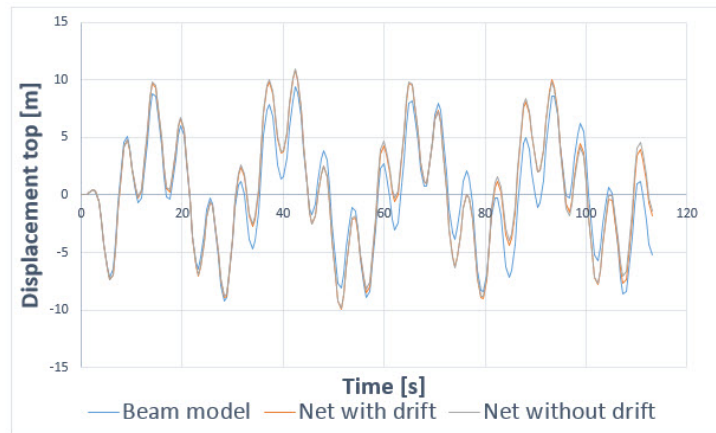
Figure 11: Comparison of motions, at the top, for the Beam model, the Net model with drift, and the Net model without drift.
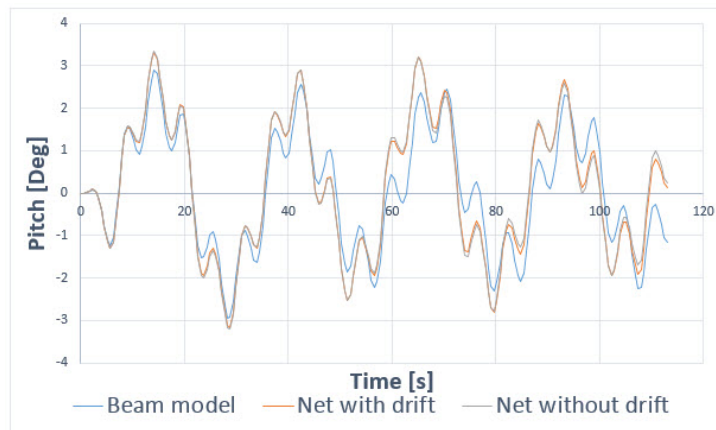
Figure 12: Comparison of rotations about the axis, normal to the flow, for the Beam model, the Net model with drift, and the Net model without drift.

As seen from Fig. 11 and Fig. 12 there is a good correspondence, between the mass and the added mass, for the Net and the Beam model. Whether one use the 2nd order terms from Eq. 14, or the 2nd order terms from Eq. 14 and Eq. 15 does not seem to have a large influence on the results in this case.

4 CONCLUSIONS

A load formulation for impermeable nets has been introduced to the Finite Element Program AquaSim. Three case studies is presented. The case studies validates the calculation of current and wave loads, and the application of mass and added mass. The case study performed on lice skirt, which deforms strongly in current, the importance of

enabling skin friction is shown. Using only form drag in the case of strong deformation leads to non-conservative results. Using a skin friction coefficient of $C_f = 0.18$, 15 % of the drag coefficient give results fitting well with the empirical data in this case. Based on the results it is hence suggested to apply a skin friction coefficient of at least $C_f = 0.18$.

For further work it is suggested to carry out more comparisons between model experiments, and numerical analysis.

Abbreviations

g	Acceleration of gravity	m/s^2
ζ	Amplitude of wave	
θ	Angle	Deg
A	Area	
J_n'	Bessel function, first derivative	
B_n	Coefficient	m
i	Complex unit (0,1)	
U_c	Current flow normal to the element	m/s
U_{tan}	Current flow tangential to the element	m/s
ρ	Density of fluid	kg/m^3
C_d	Drag coefficient	
ϵ	$\epsilon_0 = 0$ else 2	
F	Force	N
H_n^1	Hankel function, first kind	
C_l	Lift coefficient	
n	Normal vector	
C_p	Pressure coefficient	
C_s	Skin friction coefficient	
T	Time	s
h	Vertical distance	m
z	Vertical position	m
V	Volume	m^3
ω	Wave frequency	$2\pi/s$
k	Wave number	$1/m$

REFERENCES

[1] Berstad, A.J. and Heimstad, L.F. and Walaunet, J. *Model Testing of Fish Farms for Validation of Analysis Programs.* Proceedings of the ASME 2014 33rd International Conference on Ocean, Offshore and Artic Engineering OMAE2014, (June 8-13 2014), San Francisco, California. OMAE2014-24647.

[2] Berstad, A.J. and Walaunet, J. and Heimstad, L.F. *Loads from Currents and Waves on Net Structures.* Proceedings of the ASME 2012 31st International Conference on Ocean, Offshore and Artic Engineering OMAE2012, (July 1-6, 2012), Rio de Janeiro, Brazil. OMAE2012-83757.

[3] Berstad, A.J. and Tronstad, H.Y. *Design Rules for Marine Fish Farms in Norway. Calculation of the Structural Response of such Flexible Structures to Verify Structural Integrity.* Proceedings of the ASME 2004 23rd International Conference on Ocean, Offshore and Artic Engineering OMAE2004, (June 2004), Vancouver, Canada. OMAE2004-51577.

[4] Faltinsen, O.M. *Sea Loads on Ships and Offshore Structures* Cambridge University Press (1990).

[5] Lien, A.M. and Volen, Z. *Deformation of net and Permskirt and Forces on Mooring* (In Norwegian) Model experiments in flumetank. SINTEF Fisheries and Aquaculture (March 2012).

[6] MacCamy, R.C et al. *Wave Forces on Piles: A Diffraction Theory.* Corps of Engineers, Washington, D.C, (December 1954).

[7] Morison, J.R. and O'Brien, J.W. and Schaaf, S.A. *The Force Excerted by Surface Waves on Piles* Petroleum Transactions, AIME Vol. bold 189, 149-154 (1950).